Topological States in Twisted Pillared Phononic Plates

Yabin Jin[1,*], Wan Wang[1], Zhihui Wen[1], Daniel Torrent[2], Bahram Djafari-Rouhani[3]

[1]School of Aerospace Engineering and Applied Mechanics, Tongji University, 200092 Shanghai, China

[2]GROC-UJI, Institut de Noves Tecnologies de la Imatge, Universitat Jaume I, 12080, Castello, Spain

[3]Institut d'Electronique, de Microélectonique et de Nanotechnologie, UMR CNRS 8520, Département de Physique, Université de Lille, 59650 Villeneuve d'Ascq, France

[*]Corresponding author: 083623jinyabin@tongji.edu.cn

In recent years, the advances in topological insulator in the fields of condensed matter have been extended to classical wave systems such as acoustic and elastic waves. However, the quantitative robustness study of topological states which is indispensable in practical realization is rarely reported. In this work, we proposed topologically protected edge states with zigzag, bridge and armchair interfaces in a new twisted phononic plate. The robustness of non-trivial band gap in bulk structure is clearly presented versus twisted angles, revealing a threshold of 5 degrees which is the key fundamental information for the robustness of topological edge states. We further defined a localized displacement ratio as an efficient parameter to characterize edge states. Due to the different orientation of the three interfaces, zigzag and bridge edge states show higher quantitative robustness in their localized displacement ratio. A map of robustness as a function of both frequency and twisted angle highlights the better performance of the topological zigzag edge state. Robustness is evaluated for twisted angle and for all possible types of interfaces for the first time, which benefits for the design and fabrication of solid functional devices with great potential applications.

Key words: topological insulator, phononic plate, robustness, Valley Chern number

1. Introduction

Topologically protected states with single directional propagation and back scattering free properties attract increasing attention in quantum [1] and photonic [2] systems. Recently they have been extended to acoustic [3-5] and elastic [6-8] systems. Generally, Dirac cones are protected by the space inversion and the time-reversal symmetries. To obtain topological insulators, several mechanisms including the quantum Hall effect [9-11], the quantum spin Hall effect [12-19] and the valley Hall effect [4, 20-25] are proposed to open non-trivial band gaps from Dirac cones. Chern numbers of the bands above and below the opened gap can be calculated as a non-zero value revealing the topological property of the bands. Various topological protected edge states and even topological Fano resonances [26] can be realized as a consequence and they can exhibit robustness against defects, sharp bends/corners, disorders, among others. The analogue in mechanical plate system deserves special attention since it has great potential applications in solid functional devices in nano/micro scale and vibration isolation and energy harvesting in macroscale.

However, in most of the previous references, the robustness of the topological edge states was demonstrated qualitatively by introducing certain perturbations while the quantitative

investigations of their robustness remain unexplored. Recently, Jin et al quantitatively studied the robustness of topologically protected zigzag edge states in pillared phononic crystals with respect to position and geometrical parameters disorders by calculating the transmission curves and revealing that their trends exhibited a threshold with the amount of disorder [27]. Orazbayev and Fleury quantitatively analyzed topological edge modes in photonic crystals with zigzag, bridge and armchair interfaces and compared them in spin-Hall and valley-Hall insulators showing the importance of the specific edge on the robustness [28]. Deng et al systematically studied the angle dependence of topologically protected armchair edge states and revealed the difference and similarities to spin-Hall and valley-Hall effect designs [29]. For the platform of phononic plates [30-34], it is possible to design a phononic plate with double sided pillars and further twist the double layers as a Moiré pattern. Therefore, twisted angle behaves as a new perturbating degree. Despite that Moiré patterns are widely studied in bilayer of graphene, it remains unexplored in mechanical system. It will be interesting to know how topological states maintain robust in mechanical Moiré patterns and how the robustness bears for different types of interfaces.

In this work, we first study the non-trivial band gap in double sided pillared plate that possesses wider gap width than single sided case, leading to a better wave prohibition. The dependence of this non-trivial band gap with twisted angle will be consequently analyzed to offer a general view of the robustness, which plays a key role in robust topological edge states. Then, the three types of interfaces, namely zigzag, bridge and armchair, are constructed between two bulk topological media, showing different behaviors and robustness of topological edge modes. Due to different orientations, the three topological edge states exhibit different trends in localized displacement ratio curves as well as the displacement distributions. Finally, the full maps of robustness as a function of both twisted angle and frequency are provided to give a comprehensive understanding.

2. Robustness of topologically protected band gaps

We first consider a honeycomb arrangement of pillars attached to a thin elastic plate on a single side or on both sides. The entire structure is made of aluminum, whose elastic parameters are Young's modulus E = 73GPa, Poisson ratio ν = 0.17 and density ρ = 2730kgm^{-3}. It should be noted that the model can be applied to other solid materials since the physical trends and conclusions are mainly related to the geometrical parameters rather than to the material properties. The equations of motion of the solid structure are, assuming harmonic time dependence,

$$\omega^2 \rho\, u_i = \sigma_{ij,j} \qquad \text{Eq.(1a)}$$

$$\sigma_{ij} = C_{ijkl}\, u_{k,l} \qquad \text{Eq.(1b)}$$

where ω is the angular frequency, $\boldsymbol{u}$ is the displacement vector, $\boldsymbol{\sigma}$ the stress tensor and C the stiffness tensor, which for isotropic materials is a function of the Young's modulus E and Poisson ratio ν only. Einstein's summation convention has to be applied for repeated indexes. We apply Bloch boundary conditions at the boundaries of the two-dimensional unit cell that defines the periodic arrangement of pillars over the plate, and free boundary conditions at the surfaces of the solid in contact with air. The resulting eigenvalue problem is solved by the finite element method and a set of dispersion curves $\omega=\omega(\boldsymbol{k})$, with $\boldsymbol{k}$ being Bloch's wave number, are obtained and depicted normalized units Ωa defined as

$$\Omega^2 = \omega^2 \rho a^2 e / D \qquad \text{Eq.(2)}$$

where a is the lattice constant, e the thickness of the plate and $D=Ee^3/12(1-\nu^2)$ the rigidity of the plate. We will use $e=0.1a$ as the thickness of the plate in the following calculations. The radius of the pillar is $r=0.1a$. In the single-sided unit cell, the masses of the two pillars can be identical $m_{R1}=m_{R2}$ (or $h_1=h_2=1.2a$, h is the height of the pillar) or different $m_R=3m_{R2}$ ($h_1=1.2a$, $h_2=0.4a$). For double-sided unit cell, the two pairs of pillars are symmetric with respect to the middle plane of the plate. The choice of h_1 and h_2 should consider two factors: i) increasing the difference between h_1 and h_2 broadens the opened bandgap from the Dirac cone; ii) however, a change in the heights h_1 and h_2 will obviously change the resonant frequencies of the pillar (e.g. bending and compressional modes) which consequently may shift into the interested frequency range associated with the original Dirac cone and further interact with the flexural mode, resulting in several divided bandgaps. To realize a wide opened bandgap which is isolated from resonant modes, we found the choice ($h_1=1.2a$, $h_2=0.4a$) works well.

Fig.1(a) shows the full band structures of identical or different single-sided pillars in the honeycomb unit cell as marked in blue and black, respectively. Due to the spatial symmetry for identical pillars, a Dirac cone of flexural mode appears at the K point in the first Brillouin zone. The frequency of Dirac cone is related to the compressional resonant frequency of the pillars and the ratio between the mass of the pillars and that of the plate in the unit cell[35]. When the two pillars are different, e.g. $h_1=1.2a$ and $h_2=0.4a$, the inversion symmetry of the unit cell is broken while C_3 symmetry is preserved, resulting in the opening of the Dirac cone that forms a non-trivial band gap for flexural mode. For the double-sided case, the full dispersions are plotted in Fig.1(b). Since the mass ratio between pillars and the plate is double from single-sided to double sided, the frequency of the Dirac cone decreases slightly [35]. When the inversion symmetry is broken, the width of the non-trivial band gap of flexural mode is about 2 times the one in Fig.1(a). A wider band gap can support better flexural wave prohibition with less leakage into the bulk modes, which is an advantage of the double-sided pillared phononic plates. It is also found that the robustness of the topologically protected state for double-sided phononic plate can be higher than that for single-sided case (as seen the example in Fig.S1 in the Supplementary Information).

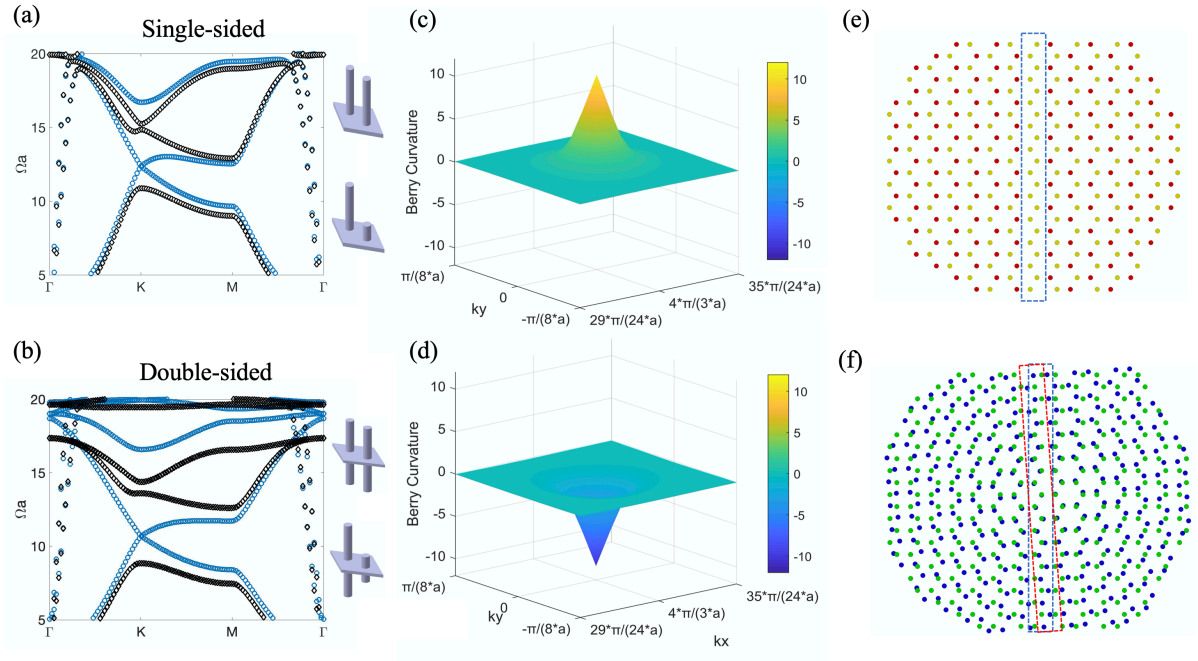

Figure 1: (a) Dispersion curves of the phononic crystal plate with single-sided pillars when the masses of two pillars in the honeycomb unit cell are equal h_1=h_2=1.2a (blue) or different h_1= 1.2a and h_2=0.4a (black). The unit cell geometries are shown on the right; (b) same as in (a) but for double-sided pillars. The unit cell geometries are shown on the right;(c) and (d) are Berry curvatures for the black bands below and above the non-trivial gap near the valley K in (b), respectively. (e) an example of the zigzag interface (marked as the dotted rectangle) between two topologically different one-sided phononic plates. The heights of the yellow and red pillars are respectively h_1=1.2a and h_2=0.4a (f) an example of the twisted double sided phononic plate with 4 twisted degrees. The two colors mean the positions of the pillar patterns in the two sides of the plate. The twisted zigzag interfaces are marked as blue and red dotted rectangles.

The valley Chern number of the lower and upper bands associated with the gap are 1/2 and -1/2 by the numerical integration of the Berry curvature over a small region around the valley K, calculated as

$$C = \frac{1}{2\pi} \int \Omega(\vec{k})\, d\vec{k} \qquad \text{Eq.(3)}$$

$\Omega(\vec{k})$ are the Berry curvatures, shown in Fig.1(c) and (d) for the two bands which are below and above the gap. The opposite valley Chern numbers are implied by band inversion mechanism, making the system support topologically protected states within the non-trivial band gap, as an elastic analog of quantum valley Hall effect. An interface can be consequently constructed by two bulk media with different orientations (as shown the zigzag interface in the dotted rectangle in Fig.1e) and topologically protected interface states can be realized. The comparison of quantum valley Hall, quantum spin Hall and quantum Hall effects analogs can be found in detailed in recent reviews [5, 8].

For double-sided pillared phononic plates, it is possible to twist the honeycomb lattice pillars on one side while keeping the other side fixed, forming a Moiré pattern as shown in Fig.1(f). From Fig.1, the absolute band gap of flexural modes maintains along any direction of the first Brillouin zone.

We construct a 12×10 superlattice of double-sided pillared phononic plates. Periodic boundary conditions are applied to the two edges of the plate along the direction of 12 units. A flexural wave is excited and out of plane displacement is integrated along a line at the exit of the superlattice. We fix pillars on one side of the plate, then twist the pillars on the other side with the origin as the center of the superlattice. The transmission is calculated as the integrated displacement ratio between pillared plate and a reference plate without pillar. Wave propagations along ΓK and ΓM directions are compared to the case when the twist angle is zero. In Fig.2 (a) and (b), the transmission diagrams as a function of the normalized frequency and twist angle are displayed, where the values of the color bar stand for the transmission. When the twist angle is 0 degree, the band gap ranges from Ωa =9.5 to Ωa =13.7 for ΓK and from Ωa =8 to Ωa =12.8 for ΓM. For twist angles larger than 5 degrees, the non-trivial band gap disappears. The twisted 5 degrees plays a threshold in robustness of the non-trivial band gap.

Increasing twist angle changes the double-sided pillared phononic plate from an insulator to a conductor for flexural waves. Since edge states are topologically protected in the non-trivial band gap, if the non-trivial band gap is disturbed, topologically protected edge states will fail to exist, showing the importance of the robustness property displayed in Fig.2.

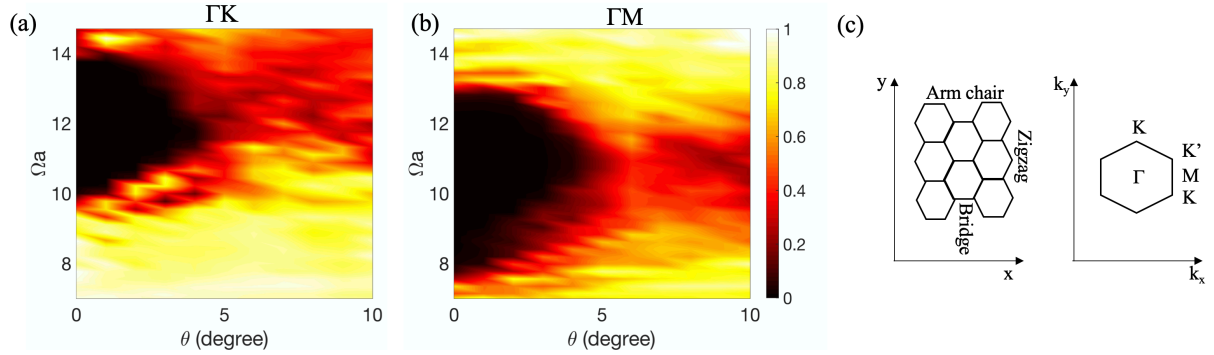

Figure 2: (a) ΓK directional transmission diagram as a function of the normalized frequency and twist angle. (b) same as in (a) but in ΓM direction. The values in the color bar mean the transmission coefficient. (c) The three boundaries (zigzag, bridge and arm chair) of the honeycomb lattice and the corresponding first Brillouin zone.

3. Robustness of topologically protected interface states

Similar to the graphene lattice, the honeycomb lattice has three types of edges, namely zigzag, bridge and armchair edges. In most previous studies, one type of edge is chosen to analyze topological edge states for acoustic and elastic waves. Here, we compare topological states among all the three edges for twisted Moiré patterns. The interface of two bulk lattices as zigzag, bridge and armchair edges are constructed in the center of a stripe with finite length in horizontal direction. The dispersions of these stripes are calculated and presented in Fig.3, where the color bar means the ratio of total displacement β in interface pillars and in all pillars

$$\beta = \frac{\iiint_{interface\ pillars} \sqrt{|u_x|^2+|u_y|^2+|u_z|^2}\,dV}{\iiint_{all\ pillars} \sqrt{|u_x|^2+|u_y|^2+|u_z|^2}\,dV} \qquad \text{Eq.(4)}$$

where u_x, u_y and u_z are the three displacement components. From Fig.3, new edge modes highlighted in colors appear in the flexural non-trivial band gaps for all three types. For zigzag and bridge interfaces which are along ΓK direction (as shown in Fig.2c), only the topologically protected edge modes exist in the band gap with highly concentrated elastic energy at the interface pillars; the armchair interface which is parallel to ΓM direction supports two light branches as well as two blue branches appearing in the band gap which are all quite flat, hence they are not expected to support sufficient robust edge propagations [28]. From the associated eigenmodes at the bottom of each dispersion curves in Fig.3, the elastic energy of the zigzag and bridge interface states is mostly concentrated at the middle interface whereas it is leakier into the bulk for the armchair case.

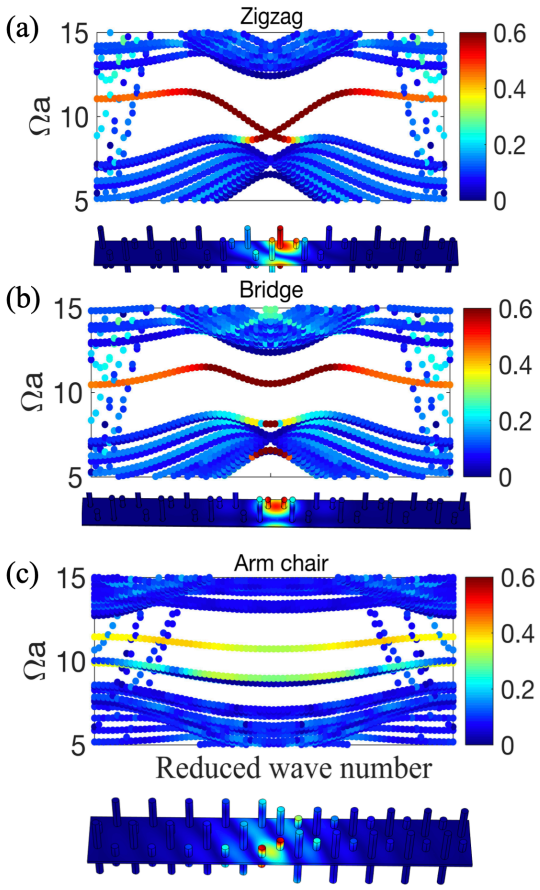

Figure 3: Edge mode dispersions for (a) zigzag (b) bridge and (c) armchair interfaces. The color bar of dispersions with the same scale represents the ratio between total displacement in the interface pillars and in all pillars. The displacement fields of the three edge modes are placed at the bottom of dispersion curves.

It is important to quantitatively investigate the robustness of edge states against perturbations in solid-state phononic device applications. The robustness against random positions and geometric parameters/resonant frequencies are already studied recently in [27, 28] . We study here this issue in Moiré pattern double-sided pillared phononic plates. For this purpose, we consider the round structure in Fig. 4 where the interface pillars are covered by the blue rectangle. Two bulk lattices I and II with different topological phases that define the interfaces are separated by the blue dotted line. A flexural wave source with finite length (out of plane force applied to a finite vertical section in the plate) is set at the left of the interface and perfectly matched layers are applied to the outer boundary of the round phononic plates to avoid any wave reflection. The red dot defines the center point around which the twisting takes place. We quantitatively calculate the localized displacement ratio Φ as

$$\Phi = \frac{\iiint_{boxed\ pillars} \sqrt{u_x^2+u_y^2+u_z^2}\,dV}{\iiint_{all\ pillars} \sqrt{u_x^2+u_y^2+u_z^2}\,dV} \qquad \text{Eq.(5)}$$

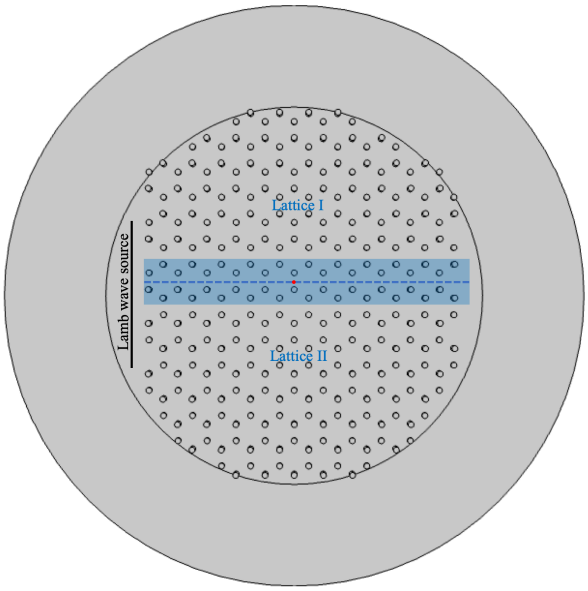

Figure 4: Adopted simulating model (zigzag interface as an example). The lattices I and II of the bulk phononic structures are separated by the dotted blue line with the interface pillars covered by the blue rectangle. The red dot is the center of twisting. A line Lamb wave source is excited at the left exit of the interface. The whole phononic structure is surrounded by a PML to avoid any wave reflection from the boundary.

We choose the normalized frequency 9.66 (zigzag),11.34 (bridge),9.91(arm chair) to analyze the robustness of interface states against different twisted angles since the three interface states are well excited at these frequencies. In the left part of Fig.5, we plot the behaviors of localized displacement ratios, then we show 4 propagating fields for each interface on the right. For zigzag interface, the localized displacement ratio first keeps stable until a twisted angle of 1°, then it slowly decreases until 3°. Between 3° and 5°, it dramatically drops from 0.85 to 0.4. Finally, it remains around 0.35 for higher twisted angles. For bridge interface, it increases a bit until 2°and significantly drops from 1.15 (2°) to 0.55 (5°), then it stays around 0.5 for higher twisted angles. For armchair interface, it almost decreases immediately and linearly from 0° to 5°with the value dropping from 1 to 0.4, then keeping stable for higher twisted angles. Given that 5° plays a threshold to change from topological insulator to conductor for flexural waves as revealed in Fig.2, the trends of the three curves in Fig.5 also support this conclusion that they all turn to small fluctuations around a constant value when the twisted angle is larger than 5°. The initial tendencies of zigzag and bridge interfaces show certain robustness as topologically protected states while the armchair interface shows less robustness.

The right part of Fig.5 exhibits propagating fields of flexural waves at 4 different twisted angles for each interface. Among the zigzag and bridge interface states, the former is more localized at the interface than the latter. Both of them show the robustness at 2°. Due to the closing of non-trivial band gap, the flexural waves distribute in the whole structure resulting in a low localized displacement ratio at 5° and 9°. Nevertheless, the interfaces can still support wave propagations. However, the armchair interface state loses the ability to support wave propagation when increasing the twisted angle.

Therefore, the results in Fig.5 reveal that the armchair interface mode shows poor robustness against twisted angle; the zigzag and bridge interface modes show high robustness until the

nontrivial band gap disappears with a threshold twist angle of 5°. Given that armchair interface directs along ΓM while zigzag/bridge interface points along ΓK, the above conclusions support the claim of different robustness at the beginning of this section.

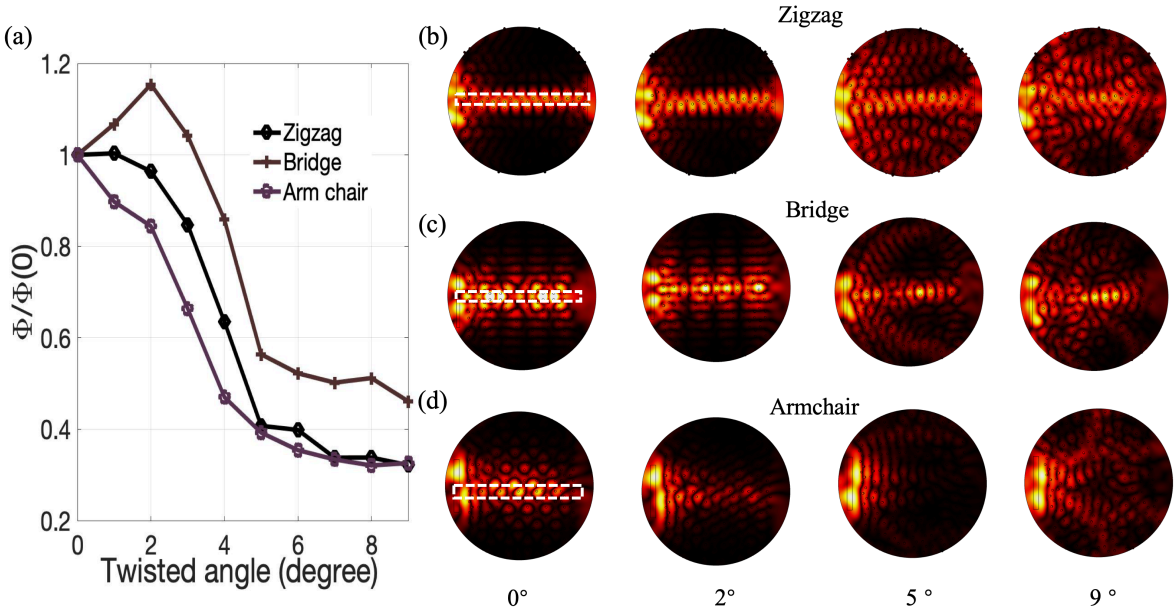

Figure 5: (a) Localized displacement ratio Φ/Φ(0) as a function of twisted angle for the three types of edges. Φ(0) is for the untwisted case (twisted angle of 0°). The flexural wave propagating states for the three types of edges at 0°, 2°, 5° and 9° are displayed at (b-d). The white dotted boxes at 0°for the three edges stand for the position of the interfaces.

The full robustness of edge states against both twisted angle and normalized frequency is calculated and similar localized displacement ratio is plotted as a 2D color maps in Fig.6 where the color bars are identically scaled to show the localized displacement ratio Φ. The zigzag edge state covers the frequency range from Ωa =9 to Ωa =11.5 at 0°, then it has a sudden shift from 4° to 5°, showing a much higher robustness than the other two interfaces. The bridge edge state is narrow band as compared to the zigzag case. The armchair edge state exhibits two highlighted bands in the 2D map being consistent with the behavior shown in Fig.3. The localized displacement ratio bands of the bridge and armchair cases in Fig.6b and 6c show a cutting edge at 5°. From the maximum color fields, the zigzag edge state is better confined than the bridge and armchair states. To conclude, the zigzag edge state shows a high robustness with broadband and highly localized properties; meanwhile, 5° plays a threshold value to all of the three interface states.

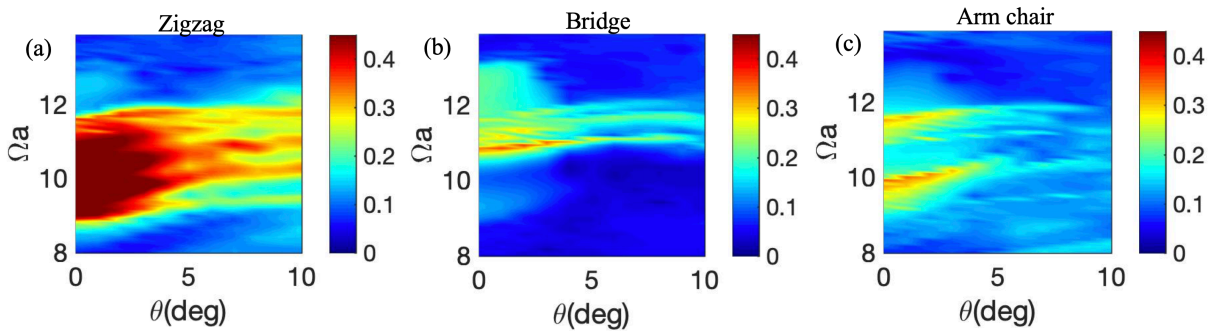

Figure 6: localized displacement ratio diagram as a function of the twist angle and the normalized frequency for (a)zigzag, (b) bridge and (c) arm chair interfaces. The color bars are identically scaled to show the localized displacement ratio.

4. Summary

In this work, we proposed a new type of phononic plate with double-sided pillars in a honeycomb array. The two sides of lattice pillars can be twisted with respect to each other resulting in a so-called Moiré pattern in this mechanical system. A non-trivial band gap is designed with the Valley-Hall effect by breaking the inversion symmetry in the unit cell. It is found that the non-trivial band gap of such double-sided phononic plate is wider than that of the single-sided case, showing a better isolation of wave propagation and confinement of edge states with less leaky effect. A sufficient large supper-lattice is constructed to study the robustness of the non-trivial band gap against twisted angle. It reveals that 5° plays a key threshold in the robustness since the non-trivial band gap will disappear when twisted angle is larger than 5°. Then we design zigzag, bridge and armchair interfaces to study their fundamental physics in topologically protected edge states. We quantitatively characterize the robustness with localized displacement ratio which is an important and useful parameter to describe edge states. Given that armchair interface directs along ΓM and zigzag/bridge interface orients along ΓK, the robustness of zigzag/bridge edge state is better than that in the armchair case as the non-trivial band gap is opened from the Dirac cone at K point. Twisted 5° is also a crucial threshold for all the three types of interfaces but with different behaviors at larger twisted angles: for zigzag and bridge edges, although the wave penetrates into bulk media, the interface propagation is still conserved; for armchair edge, the interface propagating disappears. Full quantitative maps of robustness are provided for localized displacement ratio as a function of normalized frequency and twisted angle, which are consistent with the edge modes in dispersions and shows 5° being a cut-off value for the conservation of the topological edge states. The most robust designs in both twisted angle and frequency is found as zigzag interface. The systematic quantitative robustness revealed in this study is an indispensable tool for the realization of solid devices based on topological physics not only in micro/nano scale but also in macroscale. Some possible techniques can be considered for sample fabrication in future, such as nanoimprint lithography for nanoscale, 3D printing for microscale and machining process for macroscale.

Acknowledgment

This work is supported by the project from the National Natural Science Foundation of China under Grant No.11902223, the Shanghai Pujiang Program under Grant No. 19PJ1410100, the

program for professor of special appointment (Eastern Scholar) at Shanghai Institutions of Higher Learning, the Fundamental Research Funds for the Central Universities and the High-Level Foreign Expert Program from the Ministry of Science and Technology of P.R.China. Y. Jin would like to thank Wei Wang, Lin Chen and Chao Song for their help in calculations. Daniel Torrent acknowledges financial support through the "Ramón y Cajal" fellowship under grant number RYC-2016-21188 and to the Ministry of Science, Innovation and Universities through Project No. RTI2018- 093921-A-C42.

References

[1] M.Z. Hasan, C.L. Kane, Colloquium: Topological insulators, Reviews of Modern Physics, 82 (2010) 3045-3067.
[2] A.B. Khanikaev, S. Hossein Mousavi, W.-K. Tse, M. Kargarian, A.H. MacDonald, G. Shvets, Photonic topological insulators, Nature Materials, 12 (2012) 233.
[3] C. He, X. Ni, H. Ge, X.-C. Sun, Y.-B. Chen, M.-H. Lu, X.-P. Liu, Y.-F. Chen, Acoustic topological insulator and robust one-way sound transport, Nature Physics, 12 (2016) 1124.
[4] J. Lu, C. Qiu, L. Ye, X. Fan, M. Ke, F. Zhang, Z. Liu, Observation of topological valley transport of sound in sonic crystals, Nature Physics, 13 (2016) 369.
[5] X. Zhang, M. Xiao, Y. Cheng, M.-H. Lu, J. Christensen, Topological sound, Communications Physics, 1 (2018) 97.
[6] P. Wang, L. Lu, K. Bertoldi, Topological Phononic Crystals with One-Way Elastic Edge Waves, Physical Review Letters, 115 (2015) 104302.
[7] S.H. Mousavi, A.B. Khanikaev, Z. Wang, Topologically protected elastic waves in phononic metamaterials, Nature Communications, 6 (2015) 8682.
[8] G. Ma, M. Xiao, C.T. Chan, Topological phases in acoustic and mechanical systems, Nature Reviews Physics, 1 (2019) 281-294.
[9] A.B. Khanikaev, R. Fleury, S.H. Mousavi, A. Alù, Topologically robust sound propagation in an angular-momentum-biased graphene-like resonator lattice, Nature Communications, 6 (2015) 8260.
[10] Y. Ding, Y. Peng, Y. Zhu, X. Fan, J. Yang, B. Liang, X. Zhu, X. Wan, J. Cheng, Experimental Demonstration of Acoustic Chern Insulators, Physical Review Letters, 122 (2019) 014302.
[11] H. Chen, L.Y. Yao, H. Nassar, G.L. Huang, Mechanical Quantum Hall Effect in Time-Modulated Elastic Materials, Physical Review Applied, 11 (2019) 044029.
[12] Z.-G. Chen, X. Ni, Y. Wu, C. He, X.-C. Sun, L.-Y. Zheng, M.-H. Lu, Y.-F. Chen, Accidental degeneracy of double Dirac cones in a phononic crystal, Scientific Reports, 4 (2014) 4613.
[13] Y. Deng, H. Ge, Y. Tian, M. Lu, Y. Jing, Observation of zone folding induced acoustic topological insulators and the role of spin-mixing defects, Physical Review B, 96 (2017) 184305.
[14] S. Yves, R. Fleury, F. Lemoult, M. Fink, G. Lerosey, Topological acoustic polaritons: robust sound manipulation at the subwavelength scale, New Journal of Physics, 19 (2017) 075003.
[15] M. Miniaci, R.K. Pal, B. Morvan, M. Ruzzene, Experimental Observation of Topologically Protected Helical Edge Modes in Patterned Elastic Plates, Physical Review X, 8 (2018) 031074.
[16] H. Chen, H. Nassar, A.N. Norris, G.K. Hu, G.L. Huang, Elastic quantum spin Hall effect in kagome lattices, Physical Review B, 98 (2018) 094302.

[17] J. Chen, H. Huang, S. Huo, Z. Tan, X. Xie, J. Cheng, G.-l. Huang, Self-ordering induces multiple topological transitions for in-plane bulk waves in solid phononic crystals, Physical Review B, 98 (2018) 014302.
[18] B.-Z. Xia, T.-T. Liu, G.-L. Huang, H.-Q. Dai, J.-R. Jiao, X.-G. Zang, D.-J. Yu, S.-J. Zheng, J. Liu, Topological phononic insulator with robust pseudospin-dependent transport, Physical Review B, 96 (2017) 094106.
[19] R. Chaunsali, C.-W. Chen, J. Yang, Subwavelength and directional control of flexural waves in zone-folding induced topological plates, Physical Review B, 97 (2018) 054307.
[20] R.K. Pal, M. Ruzzene, Edge waves in plates with resonators: an elastic analogue of the quantum valley Hall effect, New Journal of Physics, 19 (2017) 025001.
[21] J. Vila, R.K. Pal, M. Ruzzene, Observation of topological valley modes in an elastic hexagonal lattice, Physical Review B, 96 (2017) 134307.
[22] Z. Zhang, Y. Tian, Y. Wang, S. Gao, Y. Cheng, X. Liu, J. Christensen, Directional Acoustic Antennas Based on Valley-Hall Topological Insulators, 30 (2018) 1803229.
[23] Q. Zhang, Y. Chen, K. Zhang, G. Hu, Programmable elastic valley Hall insulator with tunable interface propagation routes, Extreme Mechanics Letters, 28 (2019) 76-80.
[24] Y. Chen, X. Liu, G. Hu, Topological phase transition in mechanical honeycomb lattice, Journal of the Mechanics and Physics of Solids, 122 (2019) 54-68.
[25] N. Lera, D. Torrent, P. San-Jose, J. Christensen, J.V. Alvarez, Valley Hall phases in kagome lattices, Physical Review B, 99 (2019) 134102.
[26] F. Zangeneh-Nejad, R. Fleury, Topological Fano Resonances, Physical Review Letters, 122 (2019) 014301.
[27] Y. Jin, D. Torrent, B. Djafari-Rouhani, Robustness of conventional and topologically protected edge states in phononic crystal plates, Physical Review B, 98 (2018) 054307.
[28] B. Orazbayev, R. Fleury, Quantitative robustness analysis of topological edge modes in C6 and valley-Hall metamaterial waveguides, Nanophotonics, 2019, pp. 1433.
[29] Y. Deng, M. Lu, Y. Jing, A comparison study between acoustic topological states based on valley Hall and quantum spin Hall effects, The Journal of the Acoustical Society of America, 146 (2019) 721-728.
[30] Y. Jin, N. Fernez, Y. Pennec, B. Bonello, R.P. Moiseyenko, S. Hémon, Y. Pan, B. Djafari-Rouhani, Tunable waveguide and cavity in a phononic crystal plate by controlling whispering-gallery modes in hollow pillars, Physical Review B, 93 (2016) 054109.
[31] Y. Pennec, B. Djafari-Rouhani, H. Larabi, J.O. Vasseur, A.C. Hladky-Hennion, Low-frequency gaps in a phononic crystal constituted of cylindrical dots deposited on a thin homogeneous plate, Physical Review B, 78 (2008) 104105.
[32] M. Rupin, F. Lemoult, G. Lerosey, P. Roux, Experimental Demonstration of Ordered and Disordered Multiresonant Metamaterials for Lamb Waves, Physical Review Letters, 112 (2014) 234301.
[33] Y. Jin, B. Bonello, R.P. Moiseyenko, Y. Pennec, O. Boyko, B. Djafari-Rouhani, Pillar-type acoustic metasurface, Physical Review B, 96 (2017) 104311.
[34] Y. Jin, Y. Pennec, Y. Pan, B. Djafari-Rouhani, Phononic crystal plate with hollow pillars connected by thin bars, Journal of Physics D: Applied Physics, 50 (2016) 035301.
[35] D. Torrent, D. Mayou, J. Sánchez-Dehesa, Elastic analog of graphene: Dirac cones and edge states for flexural waves in thin plates, Physical Review B, 87 (2013) 115143.